Desalination and Water Treatment
www.deswater.com
doi: 10.5004/dwt.2018.22973

133 (2018) 167–176
November

Recovery of phosphorus in sewage wastewater using magnetized FeOOH and superconducting magnetic separation

Yiran Li[a], Shijia Tan[b], Binbin Zhou[b], Weimin Zhang[a], Zhanxue Sun[a,*]

[a]*State Key Laboratory Breeding Base of Nuclear Resources and Environment, East China University of Technology, Nanchang, 330013 Jiangxi, China, Tel. +86-510-86596525; Fax: +86-510- 86582555; emails: szxforpaper@hotmail.com (Z. Sun), lyr2006xd@gmail.com (Y. Li), wmzhang@ecut.cn (W. Zhang)*
[b]*Department of Water Resources and Environmental Engineering, East China University of Technology, Nanchang, 330013 Jiangxi, China, emails: 619354928@qq.com (S. Tan), albin.summer@qq.com (B. Zhou)*

Received 16 January 2018; Accepted 12 August 2018

ABSTRACT

Phosphorus widely exists in municipal and industrial wastewater effluents and is the primary cause of eutrophication in aqueous environments. Sorption processes can remove phosphorus to a very low concentration and simultaneously recovery the phosphorus resources. Microscale magnetic material shows significant higher adsorption capacity than granular adsorbent. The operation cost of superconducting magnetic separation is extremely low. Therefore, in this work, FeOOH and magnetized FeOOH (Fe_3O_4@FeOOH) material was fabricated by a coprecipitation method to capture phosphate from municipal sewage wastewater. Fe_3O_4@FeOOH with different Fe_3O_4@FeOOH molar ratios was prepared. Fe_3O_4/FeOOH with the ratio of greater than 1:8 exhibited a satisfactory magnetization property (>6 emu/g), enabling rapid magnetic separation from water by a superconducting magnet and the recycling of the spent adsorbent. The Langmuir adsorption capacity of Fe_3O_4/FeOOH reached 4.6–11.7 mg/g in practical sewage wastewater after biological treatment. Fe_3O_4/FeOOH effectively removed phosphate from real wastewater from 1.8 mg/L to less than 0.1 mg/L. These results were interpreted by the ligand exchange mechanism, that is, the direct coordination of phosphate onto FeOOH by the replacement of hydroxyl groups. Fe_3O_4/FeOOH could be effectively separated from the sewage wastewater by a superconducting magnetic separator. A greater than 700 column volume was observed with 1/8Fe_3O_4/FeOOH used at 5 cm/s with a magnetic intensity of 5 T. The adsorbed phosphate could be desorbed with a NaOH treatment and the regenerated Fe_3O_4/FeOOH could be repeatedly used. $Ca_5(PO_4)_3OH$ and $Ca_5(PO_4)_3Cl$ were produced by adding $CaCl_2$ into the desorption solutions, and the P_2O_5 content was measured to be 38.25%

Keywords: Phosphate recovery; Wastewater; Magnetic ferric oxide; Superconducting magnetic separation

1. Introduction

Phosphorus (P), an essential element for living organisms, is an indispensable component of a cell structure and plays a key role in cellular metabolism. Phosphorus is one of the most important nutrients required for plant growth. Nearly all the phosphorus used in agriculture comes from phosphate rock mines. However, natural reserves of high-grade rock P are limited and running out on a global scale. Increasing attention has been paid to P recycling from secondary resources such as sewage wastewater and sludge. Various technologies are potentially applicable to P recovery from wastewater. However, technology implementation has often been economically infeasible because of the high cost of plant development, construction, and operation.

Phosphorus widely exists in municipal and industrial wastewater effluents and is the primary cause of eutrophication in aqueous environments. There are various methods for

* Corresponding author.

phosphorus removal from wastewater, such as coagulation and sedimentation, adsorption, and membrane treatment. The application of large doses of coagulants is typically required to consistently remove phosphorus in wastewater effluent to <0.5 mg/L. The use of coagulants for the removal of the total phosphorus (TP) down to very low limits can result in several problems: (1) the addition of high coagulant doses increases the volume and mass of solid residuals; (2) the addition of high coagulant doses is expensive; and (3) the addition of coagulants increases the total dissolved salt in the effluent.

Sorption processes have received significant attention, which can remove phosphorus to a very low concentration and simultaneously recovery the phosphorus resources. An ideal adsorbent for commercial application should have following characteristics: (1) high performance, (2) rapid adsorption, (3) cost-efficient, (4) environmentally nontoxic, (5) reusability, and (6) ease of separation. The effective separation of the adsorbents from water is essential for this application. Conventional sorbent applications occur in the form of column-based, membrane-based, or density-based separations. These methods usually suffer from a loss of theoretical exchange value within a practical time period allowed for separation. Additionally, the costs of producing granular or membrane sorbents are much higher.

Instead, magnetic micro/nanoadsorbents have a high surface area, tunable morphology, ease of separation after sorption, and a high efficiency. Tu [1] examines the feasibility of P removal/recovery using Fe_3O_4 nanoparticles, generated from a ferrite process. The maximum adsorption capacity was estimated to be 3.65 mg/g P at 318 K and pH 2.77. Many studies fabricated magnetic phosphorus adsorbents, such as Fe_3O_4@LDHs composites [2], magnetic chitosan microspheres [3], Fe_3O_4@ZrO_2 [4], magnetic diatomite and illite clays [5], and magnetic Fe–Zr binary oxides [6]. Magnetic adsorbents were employed as an alternative to biological nutrient removal for decreasing phosphorous in wastewater effluents containing a wide variety of competing anions.

Iron hydroxides, such as amorphous iron hydroxides, ferrihydrite, and goethite, have been intensely studied for phosphate removal due to their outstanding properties such as high adsorption capacity, large specific surface area, and hydrodynamic properties. Zelmanov et al. [7] investigated the phosphate adsorption properties of iron oxide/hydroxide nanoparticle-based agglomerates. Wang et al. studied the differences between ferrihydrite complexes and ferrihydrite–humic acid for phosphate adsorption through kinetic and isotherm experiments [8]. Clearly, iron hydroxides show great removal efficiency for phosphate. Granular iron hydroxides were widely investigated for phosphorus removal [9,10].

The granulation of powder adsorbents as filter media for flow-through use is a common method, but this method substantially reduces the surface area and, as a result, the phosphate adsorption capacity. It is known that finer particles have a higher adsorption capacity and faster kinetics because of the higher specific surface area, shorter intraparticle diffusion distance, and larger number of surface reaction sites. Therefore, an adsorbent would be the most efficient if it is employed in powder form. One of the recent approaches to overcome the difficulty in the recovery of adsorbents is to prepare nanosized magnetic composites as an adsorbent material because they are capable of being collected from water by providing an external magnetic field [11].

Previously, we have reported a novel technique for P recovery from an aqueous solution using superconducting magnetic separation. The operation cost is extremely low because the coils of superconducting magnets have no resistance below a critical temperature. This work fabricated a novel magnetized iron hydroxide Fe_3O_4@FeOOH and used superconducting magnetic separation to treat actual sewage wastewater. The phosphorus products were produced after a desorption and crystallization process.

2. Methods and materials

2.1. Preparation and characterization of Fe_3O_4@FeOOH

Fe_3O_4 magnetic particles were prepared via aqueous coprecipitation. Solutions of 0.2 M $FeCl_3$ and 0.1 M $FeSO_4$ were added into a 1 L flask. A black precipitate was formed upon the slow addition of ammonium hydroxide ($NH_3 \cdot H_2O$, 10 wt.%) at room temperature until the pH reached 7–8. The suspension was maintained at room temperature for 1 h. The resultant precipitate was separated with an external magnet and then washed three times with deionized water.

Different Fe_3O_4@FeOOH molar ratios were prepared as follows: a specific quality of Fe_3O_4 produced above was redispersed in 500 mL of a 1 M $FeCl_3$ solution under ultrasonic dispersion. FeOOH, 1/8Fe_3O_4@FeOOH, 1/4Fe_3O_4@FeOOH, and 1/2Fe_3O_4@FeOOH were prepared by controlling the molar ratios of Fe_3O_4 to FeOOH to be 0, 1/8, 1/4, and 1/2. NaOH was added dropwise into the $FeCl_3$ solution and the pH was controlled to nearly 7.0. The precipitate was separated by centrifugation and then washed three times with deionized water. Afterward, the precipitate was dried at 80°C. The dried materials were pulverized through a 200 mesh before use.

2.2. Batch experiments

The batch adsorption experiments consistently employed 500 mL of sewage wastewater in several 1 L beakers. The sewage wastewater sample was taken after A/O treatment from the Jiangyin municipal sewage wastewater treatment plant in Wuxi, Jiangsu province, China. The water quality indicators of the wastewater sample were as follows: COD 35 mg/L, BOD_5 7 mg/L, N-NH_3 4 mg/L, N-NO_3 13 mg/L, and P 1.8 mg/L.

Amounts of 0.25, 0.05, 0.1, 0.2, 0.5, 1.0, and 1.5 g of Fe_3O_4@FeOOH were added into 500 mL of wastewater. The pH was monitored during the adsorption process and showed little change. The beakers were mixed by a stirrer at speed of 200 rpm, and the temperature was maintained at room temperature, that is, approximately 25°C. The samples were collected after being mixed for 30 min and passed through a 0.45 μm membrane to analyze the P concentration.

2.3. Magnetic separation experiments

Magnetic separation was performed by using a superconducting magnet provided by Jack-Zhongke Superconducting Technology Co., Ltd, Wuxi, Jiangsu, China.

The superconducting magnetic separation system is similar to that of the previous work [12]. The central magnetic intensity was adjustable from 0 to 5.5 T. The inner diameter of the superconducting magnet was 102 mm, and its length was 690 mm. A 0.7 L reciprocating canister (100 mm length, 96 mm diameter) filled with steel wool was inserted into the superconducting magnet.

Stainless steel wools (430) were used to fill the 0.7 L magnetic separation canister mentioned earlier. The nonsmooth surface of the steel wool was designed to increase the magnetic gradient. The width and breadth of the steel wools were 0.10 and 0.07 mm, respectively. A volume ratio of 5% steel wool was used to fill the magnetic separation canister.

A certain amount of Fe_3O_4@FeOOH was added to the sewage wastewater and mixed for 30 min with a motor agitator at 200 rpm. The mixture was then pumped into the magnetic separation canister with a screw pump. The flow rate was controlled by a frequency converter that was connected to the pump and was measured by a flow meter. Samples were collected before and after magnetic separation. The TP concentrations were measured, as previously reported [12]. Briefly, the pH values of the samples were adjusted to be less than 2.0, and then the samples were vibrated for 30 min. The TP concentrations were measured after Fe_3O_4@FeOOH and phosphorous were dissolved. A 5 T magnetic field was used during the magnetic separation process.

2.4. Desorption studies and phosphorus recovery

A volume of air mixed with 1.4 L wash water was used outside of the magnetic field to washout and collect the P adsorbed on the Fe_3O_4@FeOOH. A certain concentration of NaOH was added to desorb the phosphorus from Fe_3O_4@FeOOH. The above-mentioned superconducting magnetic separator was then used to separate the Fe_3O_4@FeOOH and the P desorption solution. A different amount of $CaCl_2$ was added to the P desorption solution to fabricate the calcium-phosphorus products. The mixture was centrifuged (3,000 rpm) for 10 min to collect the calcium-phosphorus products.

2.5. Analytical methods

A phosphate analysis was conducted by an ascorbic acid method with a 721 spectrophotometer according to APHA standard methods [13]. The hysteresis loops of freeze-dried Fe_3O_4@FeOOH were measured with a vibrating sample magnetometer (VSM) (LakeShore7307, USA). The magnetic measurement sensitivity was 5×10^{-6} emu/g, and the maximum magnetic field was ±5 T. The mineral phases were analyzed with an X-ray diffractometer (Shimadzu XRD-6000) operating at 40 kV and 30 mA. The Cu Kα (l = 0.15418 nm) radiation over the range of 2 was from 10° to 80°. Fourier-transform infrared (FTIR) spectra were collected on a Vertex 70 FTIR spectrophotometer (Bruker Corporation, Germany) using a transmission model. XPS analyses were performed using ESCALAB 250Xi (Thermo Fisher Scientific, USA). An incident monochromatic X-ray beam from an Al target (15 kV, 10 mA) was focused on a 0.7 × 0.3 mm area of the surface of the sample at an angle of 45° to the sample surface.

3. Results and discussions

3.1. Characteristics of Fe_3O_4@FeOOH

Fe_3O_4 particle-based FeOOH adsorbents were developed through coating FeOOH over Fe_3O_4 particles using precipitation methods, and the characterization data of the synthesized products regarding the morphology, structure and magnetic property are summarized in Figs. 1 and 2. Fig. 1(d) shows that 1/2Fe_3O_4@FeOOH exhibits a cubic lattice structure, which is consistent with the Fe_3O_4 crystal structure. After increasing the FeOOH content, Figs. 1(a)–(c) show that the cubic lattice structures are not obvious. Instead, fine particles were observed at the rough interfaces of FeOOH, 1/8Fe_3O_4@FeOOH, and 1/4Fe_3O_4@FeOOH samples. The particle size distributions of the Fe_3O_4@FeOOH samples were similar. The mean particle sizes (D50) of FeOOH, 1/8Fe_3O_4@FeOOH, 1/4Fe_3O_4@FeOOH, and 1/2Fe_2O_4@FeOOH were 50.2, 52.2, 51.1, and 50.6 μm, respectively. FeOOH possibly aggregated with the Fe_3O_4 particles during the precipitation process. As mentioned in Section 2.1, during the preparation of FeOOH, Fe_3O_4 is dispersed in the $FeCl_3$ solution and acting as the seeds. Figs. 1(d) and (e) show FeOOH coated the Fe_3O_4 and formed a core-shell structure. The crystal structure of 1/2Fe_3O_4@FeOOH in Fig. 1(d) is clear. After the content of FeOOH increased, the cubic crystal structure of Fe_3O_4@FeOOH similar to Fig. 1(d) was not obvious.

Fig. 2(a) shows that the characteristic diffraction peaks of 1/2, 1/4, and 1/8Fe_3O_4@FeOOH at a 2θ of 30.1, 35.5, 43.1, 57.0, and 62.6 can be indexed to the (200), (311), (400), (511), and (440) planes, respectively, and are in good agreement with the cubic Fe_3O_4 phase (JCPDS card 19-0629). After coating with a FeOOH layer, the FeOOH @Fe_3O_4 particles exhibit an almost identical diffraction pattern to that of Fe_3O_4, demonstrating the formation of an amorphous FeOOH layer.

The hysteresis loops of the FeOOH, 1/8Fe_3O_4@FeOOH, 1/4Fe_3O_4@FeOOH, and 1/2Fe_3O_4@FeOOH were tested and shown in Fig. 2(b). The magnetization increased as the magnetic field improved from 0 to 5 T (1 T = 10,000 Gs), and saturation magnetization improved as the Fe_3O_4 increased. The magnetic hysteresis of the four types of materials above was not obvious and will demagnetize when removed from the magnetic field. The FeOOH materials were typically paramagnetic, and the magnetization improved as the proportion increased with magnetic intensity. The magnetization of Fe_3O_4@FeOOH increased sharply below 10,000 Gs, and increased slowly, which is similar to FeOOH in the range of 20,000–50,000 Gs. The proportion of Fe_3O_4 obviously strengthened the magnetic susceptibility of Fe_3O_4@FeOOH.

Figs. 2(c) and (d) show the Fe 2p XPS spectra, the peaks at 710.1 and 719.0 eV are related to Fe(II) and the shoulder peak at 724.4 eV is assigned to Fe(III), which suggest the coexistence of Fe(III) and Fe(II) in the Fe_3O_4@FeOOH samples [14]. As shown in Tables 1 and 2, the calculation of the peak area in core level spectra of Fe 2p provides a ratio of ferrous iron to ferric iron (Fe(II)/Fe(III)). The results indicate that the value of Fe(II)/Fe(III) increased from 1:8.33 to 1:4.48 with increased Fe_3O_4, which is close to the theoretical value. Meanwhile, the spectra of the Fe 2p and O 1s ratio on the surface showed similar results. The results indicated that the content of Fe_3O_4 on the surface of Fe_3O_4@FeOOH showed little variation from the

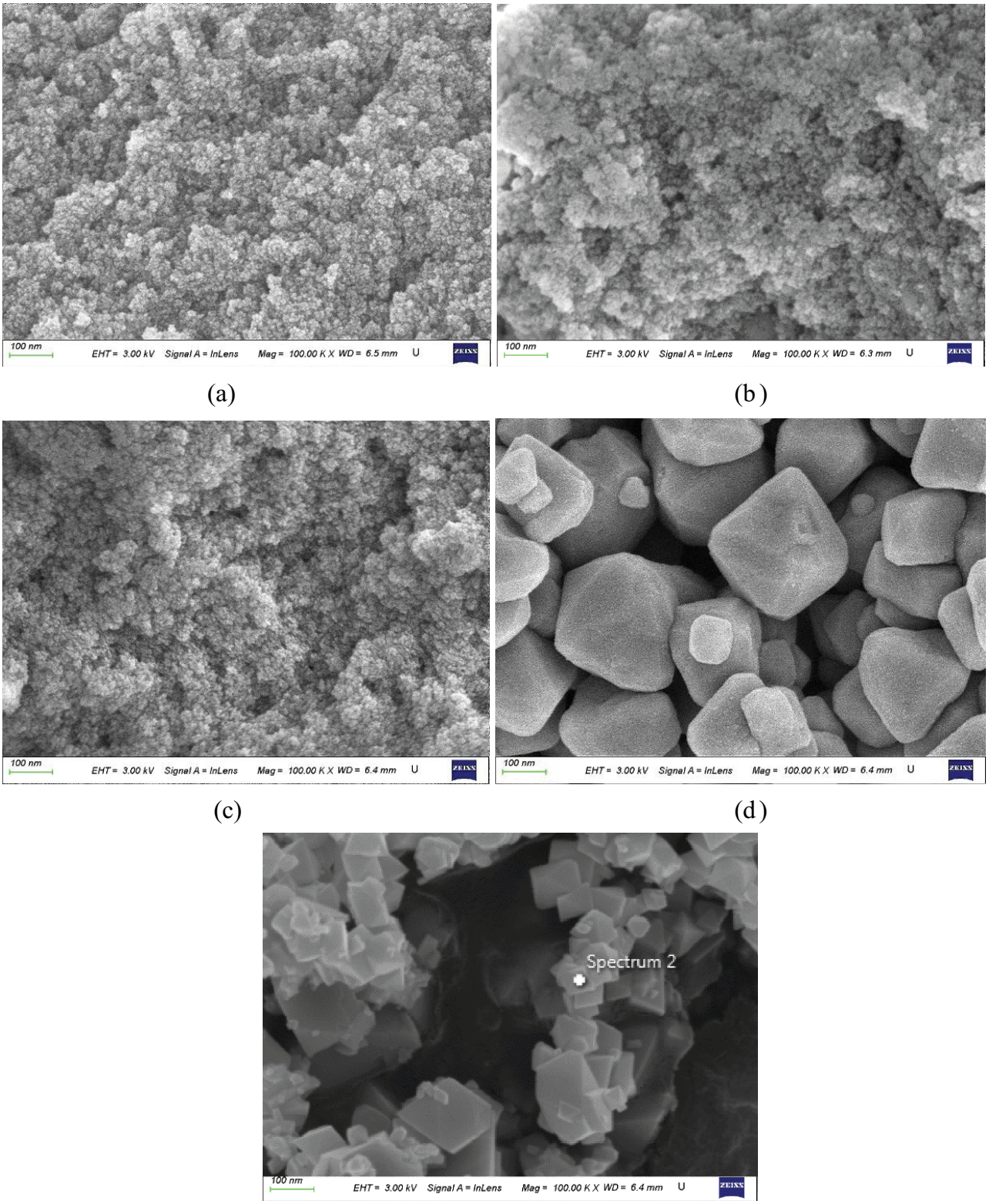

Fig. 1. SEM micrographs of FeOOH (a), 1/8Fe_3O_4@FeOOH (b), 1/4Fe_3O_4@FeOOH (c), 1/2Fe_3O_4@FeOOH (d), and Fe_3O_4 (e).

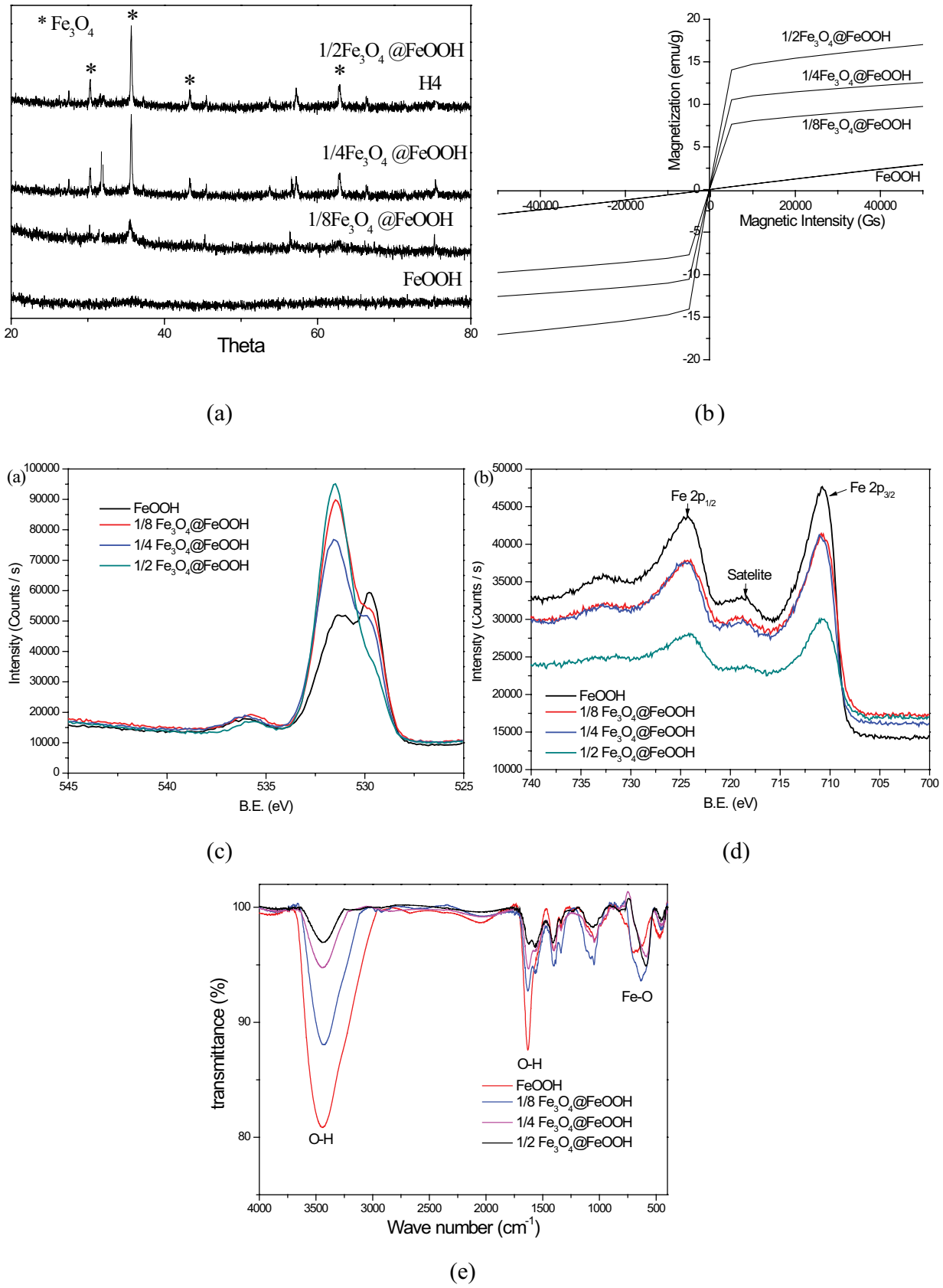

Fig. 2. XRD patterns (Cu Kα radiation) (a), hysteresis loops (b) and FTIR spectra (e) of four magnetized FeOOH powders. XPS spectra of O_{1s} (c) and Fe_{2p} (d) from the fractured surfaces of the magnetized FeOOH samples.

Table 1
XPS analysis results of O_{1s} and Fe_{2p}

	Fe_{2p}		O_{1s}		Fe:O ratio	
	B.E. (eV)	CPS·(eV)	B.E. (eV)	CPS·(eV)	Fitted value	Theoretical value
FeOOH	710.75	0.29	530.12	0.60	1:2.07	1:2.00
1/8Fe_3O_4@FeOOH	710.74	0.21	531.38	0.37	1:1.76	1:1.82
1/4Fe_3O_4@FeOOH	710.91	0.22	531.44	0.36	1:1.64	1:1.75
1/2Fe_3O_4@FeOOH	710.74	0.25	531.49	0.25	1:1.48	1:1.60

Table 2
Peak area and ratio of Fe(II) and Fe(III)

	CPS·eV		Fe(II):Fe(III) ratio	
	Fe(II)	Fe(III)	Fitted value	Theoretical value
1/8Fe_3O_4@FeOOH	19,498.08	162,484.02	1:8.33	1:10.00
1/4Fe_3O_4@FeOOH	19,904.66	132,697.70	1:6.65	1:7.00
1/2Fe_3O_4@FeOOH	13,958.54	60,689.31	1:4.48	1:4.00

inner structure. The Fe_3O_4@FeOOH fabricated in this work may be a mixture of Fe_3O_4 and FeOOH rather than a Fe_3O_4 core coated by the FeOOH structure.

FTIR spectroscopy was also used to characterize the magnetized materials and the spectra are shown in Fig. 2(d). The strong and broadband at 3,435 cm^{-1} is attributed to O–H stretch vibrations. The peak at 1,642 cm^{-1} corresponds to bending vibration of coordinated water molecules of O–H. The intensity of the O–H stretch vibrations (3,435 cm^{-1}) became weaker after the Fe_3O_4 proportion increased, which might be due to the surface occupation of Fe_3O_4. The intense absorption at 593 cm^{-1} was also observed from the Fe–O lattice vibration of Fe_3O_4. Compared with FeOOH and Fe_3O_4@ FeOOH, this further confirmed that the Fe_3O_4 occupied the surface area.

3.2. Phosphate adsorption on Fe_3O_4@FeOOH

Different dosages of Fe_3O_4@FeOOH were added into the sewage wastewater sample. The adsorption isotherms were studied at room temperature (298 K) and the results are shown in Fig. 3. By fitting the isotherm data to the Langmuir model, the parameters and correlation coefficients could be obtained, and the results are listed in Table 3. The model could be represented as the following equations:

$$q_e = \frac{q_{\max} b C_e}{\left(1 + bC_e\right)}$$

where b is the Langmuir constant in L/mg and $q_{\max}$ is the maximum adsorption capacity calculated by the Langmuir model in mg/g.

Isotherm data were well fitted to the Langmuir model in Table 3. The $q_{\max}$ of the four types of Fe_3O_4@FeOOH samples were all calculated to be less than 12 mg/g, which should be underestimated due to the low P concentration of the 1.8 mg/L sewage wastewater was used in the batch experiments. However, this calculated $q_{\max}$ value was according to the practical situation and could guide the advanced dephosphorization from sewage wastewater. In the previous

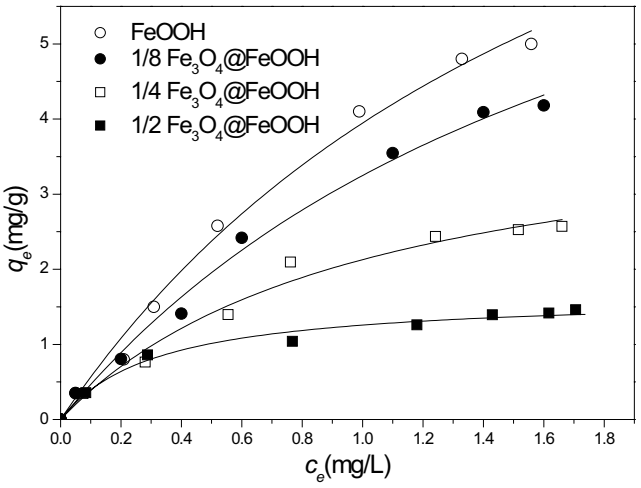

Fig. 3. Adsorption isotherm for FeOOH (open circles), 1/8Fe_3O_4@FeOOH (closed circles), 1/4Fe_3O_4@FeOOH (open squares), and 1/2Fe_3O_4@FeOOH (closed squares). Amounts of 0.25, 0.05, 0.1, 0.2, 0.5, 1.0, and 1.5 g of adsorbent were added to sewage wastewater. The initial P concentration was 1.8 mg/L.

work [15], P concentration in the simulated wastewater was reduced from 10 mg/L to less than 0.05 mg/L with 1.5 g/l FeOOH added. The objective of this work is to investigate a practical method to recovery P from actual municipal wastewater. Therefore, the P concentration was not artificially changed. The adsorption capacity of Fe_3O_4@FeOOH was about 12 mg/g in treating the 1.8 mg/L P contained wastewater. Fe_3O_4@FeOOH should be effective in treating the wastewater with P concentration higher than 1.8 mg/L by increasing the adsorbent dosages.

Phosphate adsorption onto FeOOH has been widely reported. FeOOH is believed to be an effective adsorbent for P uptake. The most commonly referenced mechanism is surface complexation modeling [16]. The adsorption of anions such as PO_4^{3-}, HPO_4^{2-}, and $H_2PO_4^-$ onto FeOOH is known to

Table 3
Calculated q_{max} and b of different adsorbents

	R^2	q_{max} (mg/g)	b
FeOOH	0.99	11.7	0.51
1/8Fe_3O_4@FeOOH	0.99	8.4	0.51
1/4Fe_3O_4@FeOOH	0.98	7.1	3.14
1/2Fe_3O_4@FeOOH	0.98	4.6	0.99

occur via specific and/or nonspecific adsorption. Specific adsorption involves ligand exchange reactions in which anions displace OH and/or H_2O from the surface. Nonspecific adsorption involves Coulombic forces and primarily depends on the pH of the sorbent [17]. It is well known that the OH^- on the surface of HFO plays an important role in P adsorption.

3.3. Phosphorus treatment by Fe_3O_4@FeOOH and magnetic separation

As discussed in Section 3.2, the adsorption capacity of the Fe_3O_4@FeOOH decreased as the Fe_3O_4 content increased. To reduce the P concentration from 1.8 to less than 0.1 mg/L, quantities of 4, 6, 7, and 8 g/L of FeOOH, 1/2Fe_3O_4@FeOOH, 1/4Fe_3O_4@FeOOH, and 1/8Fe_3O_4@FeOOH, respectively, was added to the sewage wastewater. The amounts of magnetic adsorbents captured in the canister were limited, and then determined the P content in the canister.

As reported in the previous work, steel wool filled the magnetic canister to capture the magnetized adsorbents with P adsorbents [12]. Steel wool was used to disturb the magnetic lines and thus greatly increased the magnetic gradient around the wool. The magnetized adsorbents were captured at the high magnetic gradient site, which is called the "pick-up zone" during high-gradient magnetic separation [18]. The amounts of magnetized adsorbents captured in the "pick-up zone" were limited and depended on the magnetic field, gradient, flow rate, magnetization of adsorbents, etc. Therefore, similar to granular adsorbents used in a column, there should be breakthrough curves when magnetized adsorbents were separated in the magnetic canister.

The breakthrough curves of different adsorbents captured in the magnetic canister are shown in Fig. 4. Before the leakage point of the breakthrough curve, the capture efficiencies of Fe_3O_4@FeOOH or FeOOH were nearly 100%.

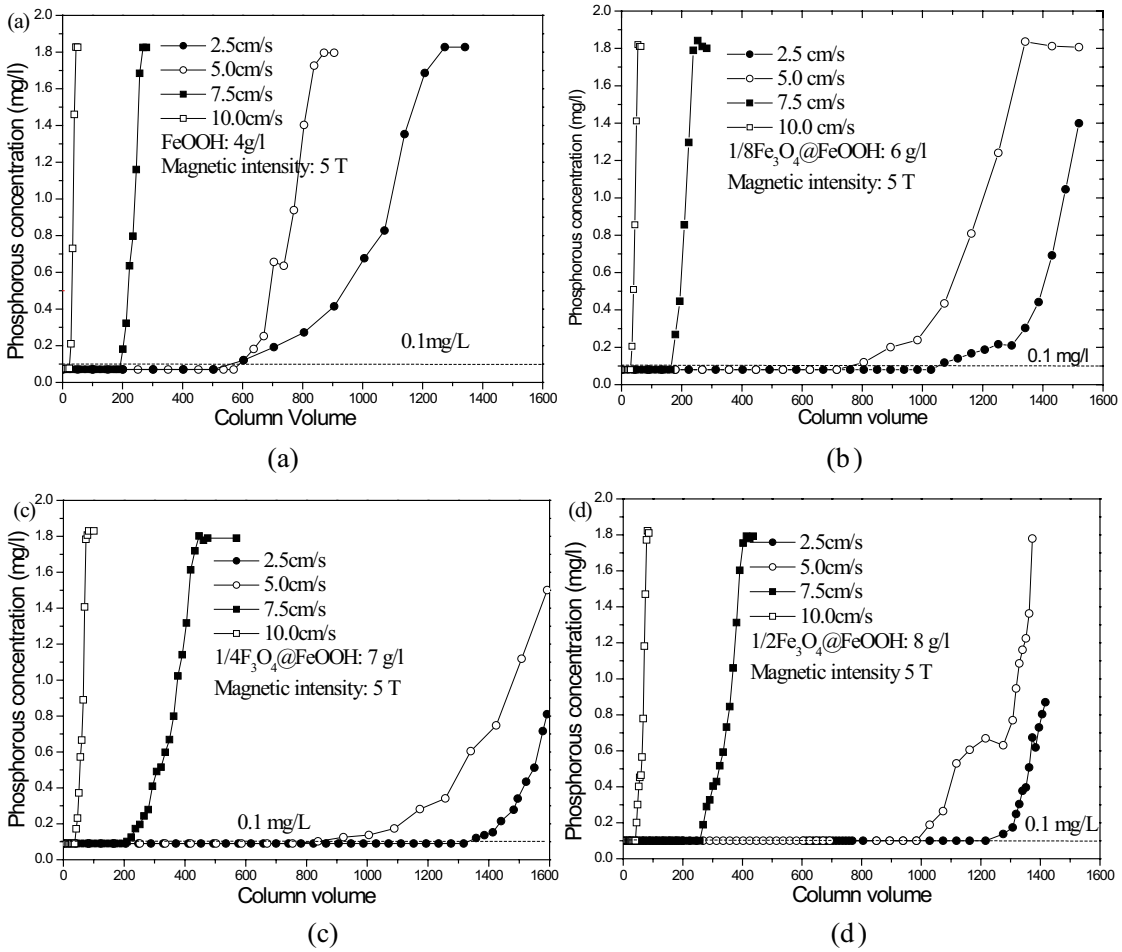

Fig. 4. Breakthrough curves of FeOOH (a), 1/8Fe_3O_4@FeOOH (b), 1/4Fe_3O_4@FeOOH (c), and 1/2Fe_3O_4@FeOOH (d) in the magnetic canister with a filtration rate of 2.5 (closed circles), 5.0 (open circles), 7.5 (closed squares), and 10.0 (open squares) cm/s at a 5 T magnetic field.

The calculated breakthrough column volume ranged from <20 to >1,000. Increasing the flow rate from 5 to 7.5 cm/s significantly decreased the breakthrough column volume. Table 4 shows the calculated phosphorus content in the canister after 5 cm/s magnetic separation by using different adsorbents. The captured P content in different canister increased from 714 to 1,190 mg in a single separation cycle with Fe_3O_4 increased. High P content in the canister was advantaged for the P desorption process.

3.4. P desorption

Five column volume, 0.1 M NaOH (170 mL) was added into the magnetic canister to desorb P. The P concentration of the desorption solution is positively correlated with the P content in the canister. A high P concentration in the magnetic canister helped to obtain a high concentration P desorption solution. As shown in Table 4, P desorption rates of different adsorbents were similar and ranged from 98.34% to 98.57%.

As shown in Table 4, the P concentration of the desorption solution increased from 0.2 to 0.33 g/L after the magnetization process of the adsorbents. The calcium concentration significantly affects the phosphorus recovery rate. A 3.0 Ca/P molar ratio leads to more than an 80% P recovery in the products. Increasing the P concentration in the desorption solution from 0.2 to 0.33 g/L improved the P recovery from 82% to 89%. High P concentration in the desorption solution was advantaged to increase the P recovery and reduce the calcium dosages.

As shown in Fig. 5, $Ca_5(PO_4)_3OH$ and $Ca_5(PO_4)_3Cl$ were identified the main mineral phases in the P products. The total P_2O_5 content was measured to be 38.25 wt.% in the P products, which meets the requirement of a first-grade product of the phosphate ore industry standards HG/T2673-1995 and HG/T2675-1995. Therefore, the P products from magnetic separation were reutilized after treating the sewage wastewater.

3.5. Phosphorus migration and transformation

Technological flow sheet of the superconducting magnetic separation for P treatment and recovery is shown in Fig. 6. FeOOH or Fe_3O_4@FeOOH was added into the sewage wastewater after biological nitrogen treatment. The TP concentration was 1.81 mg/L after the sedimentation tank. An amount of 4 kg/t Fe_3O_4@FeOOH was added prior to the superconducting magnetic separator, which was mixed with the sewage wastewater in a water tube. The nonmagnetic content of superconducting magnetic separator was treated water with a phosphorus concentration less than 0.1 mg/L. The magnetic proportion was FeOOH or Fe_3O_4@FeOOH that contained phosphorus. After the desorption and crystallization processes, there should be approximately 5 kg P products (38.25%, P_2O_5%) per 500 t sewage wastewater.

Table 4
Relationships between the breakthrough column volume and P desorption concentration and rate

	Breakthrough column volume	P concentration in the desorption solution (g/L)	P desorption rate (%)	Calculated phosphorus content in the canister (mg)
FeOOH	600	0.20	98.57	714
1/8Fe_3O_4@ FeOOH	700	0.23	98.45	833
1/4Fe_3O_4@ FeOOH	800	0.27	98.53	952
1/2Fe_3O_4@ FeOOH	1,000	0.33	98.34	1,190

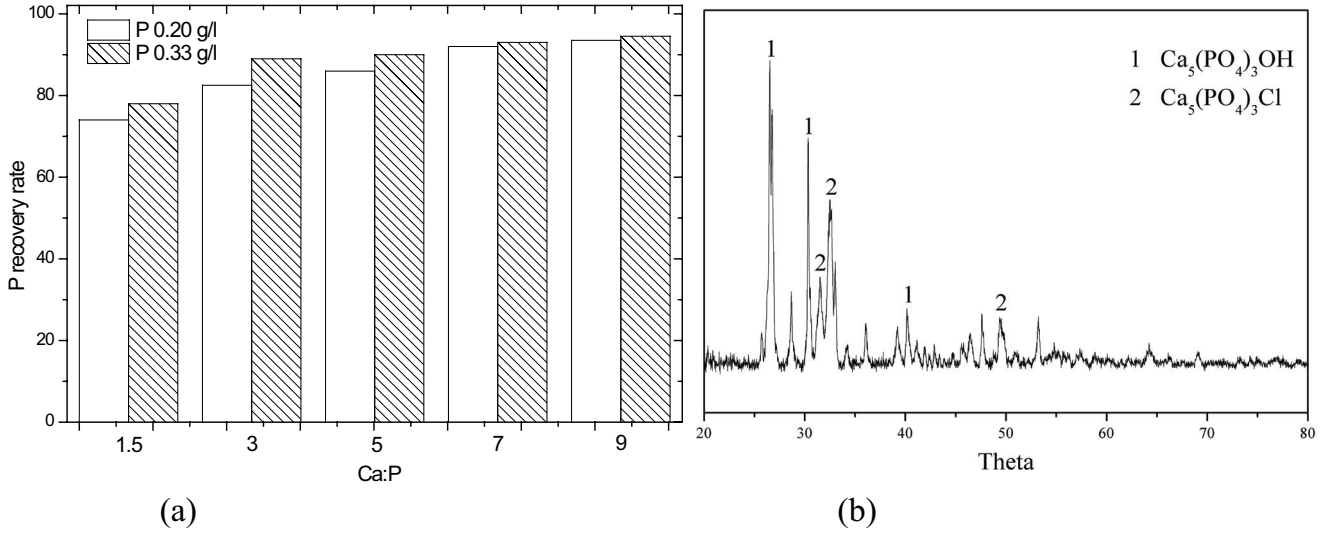

Fig. 5. Recovery rates of P at different Ca:P ratios (a) and the XRD patterns of the P products (b).

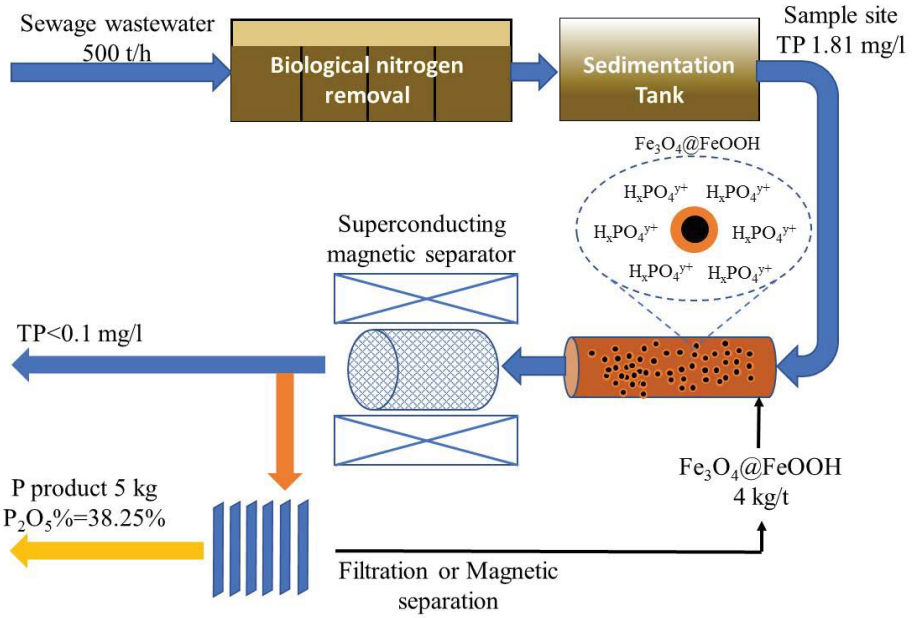

Fig. 6. Technological flow sheet of the superconducting magnetic separation for P treatment and recovery.

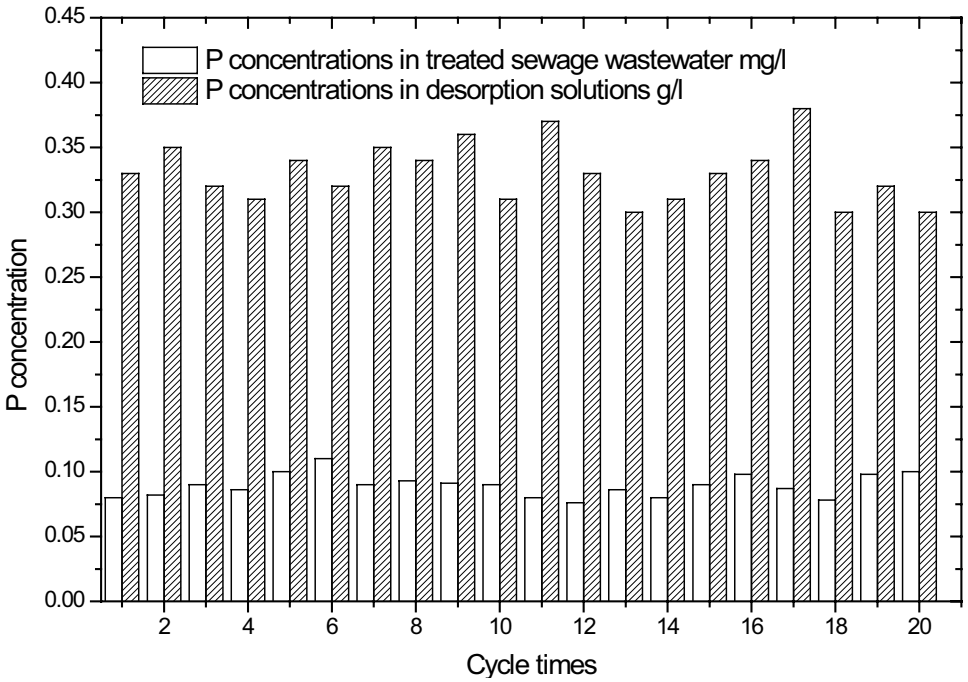

Fig. 7. P concentrations in treated sewage wastewater (mg/L) and desorption solutions (g/L) after 20 cycles. 1/2Fe_3O_4@FeOOH was used and the column volume of the magnetic separation was controlled to be 1,000. The flow rate was 5.0 cm/s and the magnetic intensity was 5 T.

3.6. Multiple cycles of sorption/desorption experiments

Fig. 7 shows the values of the P concentration in treated wastewater fluctuated and maintained to be less than 0.1 mg/L in 20 cycles. Superconducting magnetic separation combined with 1/2Fe_3O_4@FeOOH was effectively to control the sewage wastewater to be lower than 0.1 mg/L. Meanwhile, the desorption P concentration maintained at higher than 0.3 g/L. The desorption efficiency of phosphorus adsorbed on FeOOH was particularly high. The structure of FeOOH was stable during both the adsorption and desorption processes.

4. Conclusions

Fe_3O_4@FeOOH materials with different Fe_3O_4/FeOOH ratios were fabricated by a coprecipitation method to capture phosphate from sewage wastewater. With a decreasing Fe_3O_4/FeOOH molar ratio, the magnetization decreased, whereas the adsorption capacity of phosphate increased. Fe_3O_4@FeOOH enabled rapid magnetic separation from water using a superconducting magnet and the recycling of the spent adsorbent. Fe_3O_4/FeOOH effectively removed phosphate from real wastewater from 1.8 mg/L to less than 0.1 mg/L. Breakthrough curves of superconducting magnetic separation were described. High breakthrough column volume helped to improve the treatment capacity and the P desorption concentration. The adsorbed phosphate could be desorbed with a NaOH treatment and the regenerated Fe_3O_4/FeOOH could be repeatedly used. $Ca_5(PO_4)_3OH$ and $Ca_5(PO_4)_3Cl$ were produced by adding $CaCl_2$ into the desorption solutions, and the P_2O_5 contents were measured to be 38.25%.

Acknowledgments

We gratefully acknowledge Jack-Zhongke of Superconducting Technology Co., Ltd. for providing the superconducting magnet. Financial support was provided by the National Natural Science Foundation of China (no. 41772266 and 41867021), Natural Science Foundation of the Jiangxi province (no. 20171BAB206048).

References

[1] Y.J. Tu, C.F. You, C.K. Chang, M.H. Chen, Application of magnetic nano-particles for phosphorus removal/recovery in aqueous solution, J. Taiwan Inst. Chem. Eng., 46 (2015) 148–154.
[2] L.G. Yan, K. Yang, R.R. Shan, T. Yan, J. Wei, S.J. Yu, H.Q. Yu, B. Du, Kinetic, isotherm and thermodynamic investigations of phosphate adsorption onto core-shell FeOOH@LDHs composites with easy magnetic separation assistance, J. Colloid Interface Sci., 448 (2015) 508–516.
[3] M. Xiu-Ling, C. Sheng, Z. Si-Ning, Synthesis and characterization of magnetic chitosan microspheres, J. Fujian Normal Univ., 20 (2004) 62–65.
[4] Z. Wang, W. Fang, M. Xing, D. Wu, A bench-scale study on the removal and recovery of phosphate by hydrous zirconia-coated magnetite nanoparticles, J. Magn. Mater., 424 (2017) 213–220.
[5] J. Chen, L.G. Yan, H.Q. Yu, S. Li, L.L. Qin, G.Q. Liu, Y.F. Li, B. Du, Efficient removal of phosphate by facile prepared magnetic diatomite and illite clay from aqueous solution, Chem. Eng. J., 287 (2016) 162–172.
[6] F. Long, J.L. Gong, G.M. Zeng, L. Chen, X.Y. Wang, J.H. Deng, Q.Y. Niu, H.Y. Zhang, X.R. Zhang, Removal of phosphate from aqueous solution by magnetic Fe–Zr binary oxide, Chem. Eng. J., 171 (2011) 448–455.
[7] G. Zelmanov, R. Semiat, Iron (Fe^{+3}) oxide/hydroxide nanoparticles-based agglomerates suspension as adsorbent for chromium (Cr^{+6}) removal from water and recovery, Sep. Purif. Technol., 80 (2011) 330–337.
[8] H. Wang, J. Zhu, Q. Fu, H. Hu, Adsorption of phosphate on pure and humic acid-coated ferrihydrite, J. Soils Sediment, 15 (2015) 1500–1509.
[9] P.L. Sibrell, T. Kehler, Phosphorus removal from aquaculture effluents at the Northeast Fishery Center in Lamar, Pennsylvania using iron oxide sorption media, Aquac. Eng., 72–73 (2016) 45–52.
[10] M. Kunaschk, V. Schmalz, N. Dietrich, T. Dittmar, E. Worch, Novel regeneration method for phosphate loaded granular ferric (hydr)oxide – a contribution to phosphorus recycling, Water Res., 71 (2015) 219–226.
[11] Z. Wang, M. Xing, W. Fang, D. Wu, One-step synthesis of magnetite core/zirconia shell nanocomposite for high efficiency removal of phosphate from water, Appl. Surf. Sci., 366 (2016) 67–77.
[12] Y. Li, B. Zhou, F. Xu, H. Jiang, W. Zhang, The advantages of a superconducting magnetic intensity greater than 1 T for phosphate–ferric flocs separation in HGMS, Sep. Purif. Technol., 141 (2015) 331–338.
[13] A. APHA, WEF, Standard Methods for the Examination of Water and Wastewater 20th ed.-4500-NO3-D nitrate Electrode Method, American Public Health Association, Washington, DC, 1998.
[14] T. Yamashita, P. Hayes, Analysis of XPS spectra of Fe^{2+} and Fe^{3+} ions in oxide materials, Appl. Surf. Sci., 254 (2008) 2441–2449.
[15] H.A. Mengistu, A. Tessema, M.B. Demlie, T.A. Abiye, O. Royset, Surface-complexation modelling for describing adsorption of phosphate on hydrous ferric oxide surface, Water S.A., 41 (2015) 157–167.
[16] Y. Li, Z. Li, F. Xu, W. Zhang, Superconducting magnetic separation of phosphate using freshly formed hydrous ferric oxide sols, Environ. Technol., 38 (2017) 377.
[17] M. Sujana, G. Soma, N. Vasumathi, S. Anand, Studies on fluoride adsorption capacities of amorphous Fe/Al mixed hydroxides from aqueous solutions, J. Fluorine Chem., 130 (2009) 749–754.
[18] A. Cieśla, Practical aspects of high gradient magnetic separation using superconducting magnets, Physicochem. Probl. Mi., 37 (2003) 169–181.